Miniature Microwave RF MEMS Tunable Waveguide Filter

Derek Scarbrough[1], Charles Goldsmith[1], John Papapolymerou[2], and Yuan Li[2]

[1]*MEMtronics Corporation, Plano, TX, 75075, USA*

[1]dscarbrough@memtronics.com

[3]cgoldsmith@memtronics.com

[2]*Georgia Institute of Technology, Atlanta, GA, 30308, USA*

[2]john.papapolymerou@ece.gatech.edu

yuanli@ece.gatech.edu

***Abstract*— This paper presents an RF MEMS tunable filter implemented in waveguide. A compact waveguide topology was chosen to make use of high-Q cavity resonators for the creation of a low-loss, two-pole filter. The filter results in an insertion loss of 4.7-5.8 dB over the tuning range 10.12-10.33 GHz with a relative bandwidth of 0.42-0.67%. This design demonstrates an unloaded quality factor of 169-319 over the tunable frequency range with the potential to exceed 500.**

I. INTRODUCTION

As the electromagnetic environment becomes more populated, frequency-agility and narrow operating bandwidths are becoming highly desirable characteristics for bandpass filters in RF front ends. As such, bandpass filters having a high unloaded quality factor (Q_u) are a requirement for maintaining low insertion loss and minimum noise figure. To date, however, the low quality factors of lumped capacitors and inductors at low frequencies and transmission media at high frequencies have typically limited the overall Q_u factor for miniaturized planar tunable filters.

Tunable filters based on radio frequency micro-electromechanical systems (RF MEMS) technology provide the ability to create low-loss, high-linearity tuning while simultaneously reducing volume, weight, and parts count. On DARPA's UltraComm Program, the use of MEMS tunable filters in the 80 MHz to 2.8 GHz frequency range demonstrated the functionality of switched filter banks while reducing the volume by 60x, the parts count by 14x, and the weight by 150x [1].

Several examples of RF MEMS tunable filters operating from X-band to K-band have been reported [2-6]. An analysis of the published results indicates an average Q_u factor of 25-75 with an average fractional bandwidth of 6.6-11%. In [7], a suspended stripline MEMS-tunable filter achieved a Q_u of 50-150 over the frequency range 1.6-2.4 GHz with a fractional bandwidth of 10.1-12.2%. Reference [8] reports on a coupled microstrip MEMS-tunable filter constructed on an ultra low-loss substrate operating in Ku-band which achieved a Q_u of 271 with a fractional bandwidth of 13.4%. As requirements continue to call for smaller fractional bandwidths (<2%), maintaining a reasonable insertion loss will become increasingly difficult.

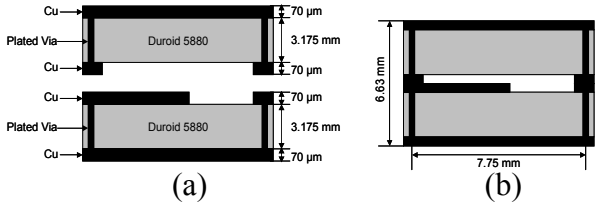

Fig.1. Cross sectional view of substrate integrated folded waveguide filter (a) pre-assembled, constituent parts and (b) assembled view.

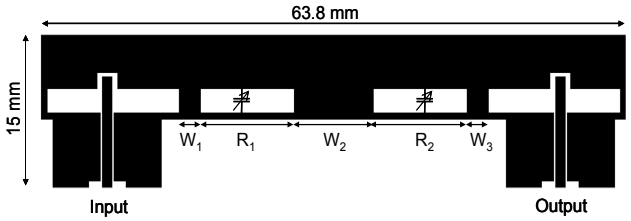

Fig.2. Top-down view of middle metallization layer for 2-pole substrate integrated folded waveguide filter.

This paper presents a two-pole, tunable filter operating over the frequency range 10.12 GHz to 10.33 GHz with bandwidths of 44 MHz – 69 MHz (0.42% - 0.67%) and a Q_u of 169-319. A compact waveguide media, whose cross-sectional area has been reduced by 78% from that of a standard rectangular waveguide, combined with low-loss capacitive RF MEMS switches were used to maximize the Q_u factor. The filter makes use of a unique tuning technique to change the resonant frequency of inductively coupled, high-Q cavity resonators. Prototype results indicate the possibility for Q_u ~500.

II. FILTER DESIGN

A second-order, Chebyshev tunable filter has been designed to operate in the X-band having a tunable frequency range 9.8-10.2 GHz with a bandwidth of 100 MHz (Figs 1, 2). Two bits of tuning using four capacitive RF MEMS switches provide for four operating states. The primary goal for this filter was to implement a MEMS-tunable filter within low-loss waveguide utilizing planar fabrication techniques to improve the Q_u factor while simultaneously reducing the volume normally associated with waveguide at X-band frequencies.

A common type of waveguide filter is the direct-coupled cavity resonator filter [9]. One variation of this category of filters, the E-plane filter, utilizes inductive discontinuities (septums) to directly couple half-wavelength cavity resonators [10]. A model describing impedance versus septum width was developed using Ansoft's High Frequency Structure Simulator. The basic circuit design developed using the g-parameters associated with a 0.1 dB pass band ripple, Chebyshev filter and frequency-dependent inverter theory is shown in Fig. 3, and consists of three K-inverters of specified impedance separated by two half wavelength cavity resonators. The filter is designed for the highest frequency desired and is tuned to lower frequencies. Each of the cavities comprising the filter resonates when half of the guided wavelength is equal to the electrical length of the cavities. Tuning is accomplished by modifying the electrical length of each of the cavities so as to change their resonate frequencies. To maintain the filter characteristics in each state, both cavities are tuned simultaneously.

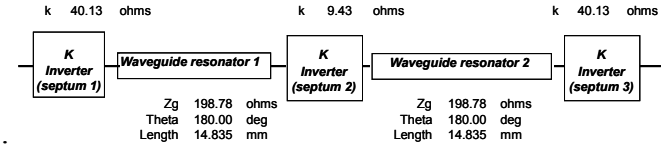

Fig.3 Ideal, 2-pole, Chebyshev, E-plane filter circuit.

Standard metal rectangular waveguide is not suitable for planar batch fabrication nor is its size desirable for a number of applications. As a result, a substrate-integrated version of folded waveguide (SIFW) was chosen as the filter platform [11]. Fig. 4 graphically compares conventional rectangular waveguide and SIFW. Folding a rectangular waveguide along the broad wall (E-field maximum) results in an exaggerated ridged waveguide configuration called a folded waveguide whose cross sectional area is approximately one-quarter of the original rectangular waveguide. The most important aspect of the folded waveguide is that the E-plane, or the plane of the electric field maximum, is in an orientation that planar fabrication techniques can exploit (Fig. 5). All processing takes place on the surface of one substrate which forms half of the filter's cross section. Afterwards, a second substrate forming the other half of the filter's cross section mates with the first; sandwiching the filter elements (Fig.1). The waveguide sidewalls are formed by periodically spaced through-wafer vias creating the electromagnetic equivalent of solid-conducting sidewalls. The result is an E-plane filter implemented in dielectrically-loaded folded waveguide with a cross-sectional area less than one quarter that of conventional WR-90. A detailed description of a filter designed in folded waveguide is found in [12].

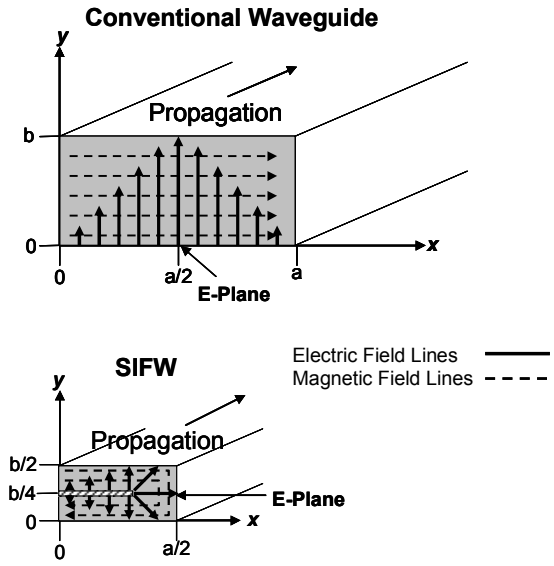

Fig.4. Cross-sectional view showing fundamental TE_{10} mode for a conventional rectangular waveguide and SIFW.

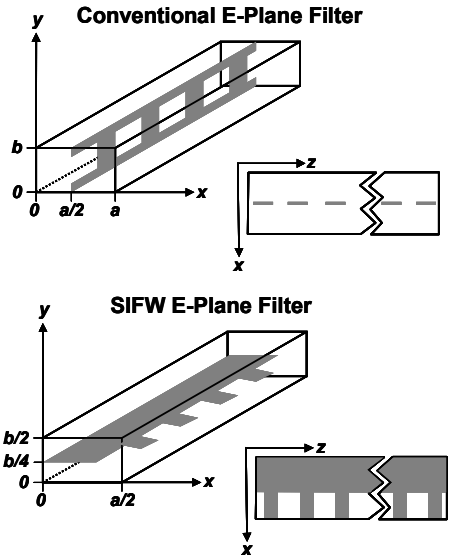

Fig.5. Comparison of an E-plane filter implementation in conventional rectangular waveguide and SIFW.

A metal stub, oriented parallel to the E-plane but not extending fully across the waveguide, is modeled as a shunt capacitor whose capacitance value depends upon the length it protrudes into the waveguide. This capacitive discontinuity can be placed within a cavity resonator to reduce the resonant frequency. Stubs are placed within each of the coupled cavity resonators that form the E-plane filter. RF MEMS switches are used to couple/decouple these stubs. When the MEMS switch is actuated, coupling the stub to ground, the resulting shunt capacitance lowers the impedance of the waveguide and reduces its phase velocity. This behavior makes the resonators appear electrically longer and, therefore, shifts the resonate frequency lower. Each tuning bit requires one stub in each resonator section. The designed filter has two poles and two bits of tuning resulting in four tuning stubs and four RF

MEMS switches. Because of the off-state capacitance of the MEMS switches (~50fF), the tuning stubs are never completely decoupled resulting in a frequency shift for the zero state. This is easily corrected by slightly pre-shortening each of the resonator lengths.

The transitions into and out of the waveguide filter include a coaxial-to-CPW transition via an end launch printed circuit board SMA connector and a CPW-to-waveguide transition via an E-plane probe located a quarter-wavelength from the back short of the waveguide. Bias lines used to actuate each of the RF MEMS switches are routed directly through the sidewall of the waveguide structure. A 1 MΩ chip resistor is included in each bias path to decouple the RF signal.

III. Fabrication

The designed filters were fabricated on 0.125 inch Rogers Duroid 5880 (ε_R = 2.2 and tanδ = 0.0009) clad in 2 oz. copper. The plated via diameter and spacing used were 0.45 mm and 1.2 mm. All metal surfaces were plated with soft gold to allow for wirebonding. The filters were fabricated in a standard printed circuit board shop.

While this filter could be monolithically constructed with fully integrated RF MEMS switches, this demonstration relied upon a hybrid assembly in which individual chips containing RF MEMS switches were fixed in place with epoxy and all electrical connections were made with wirebonds. The capacitive RF MEMS switches used are a product of a process developed at MEMtronics Corporation and are similar in design and function to the switches detailed in [13].

Both fixed- and tunable-filters were fabricated (Figs. 6, 7). Fixed-filters were created to simulate a MEMS-tuned filter. The tuning stubs for the fixed-filters are "hardwired," permanently at ground potential. These filters were used as a diagnostic tool to evaluate the impact on performance resulting from the inclusion of bias lines and RF MEMS switches.

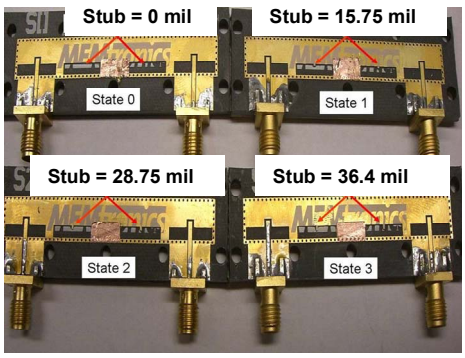

Fig.6. Fabricated fixed filters used to simulate 4 states of tunable filter.

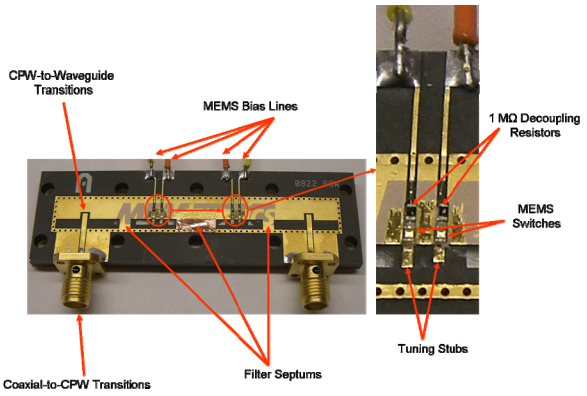

Fig.7. Fabricated and assembled RF MEMS tunable waveguide filter.

IV. Measurement Results

A. Fixed Filters

S-parameter measurements were taken on an Agilent VNA using a precision 3.5 mm calibration kit. The filter center frequencies range from 10.03 to 10.37 GHz with absolute bandwidths of 37 to 50 MHz. The unloaded Q for these devices ranged from 510 to 651. Measured insertion loss and return loss are shown in Fig. 8 and summarized in Table I. Bandwidths determined according to 10 dB return loss bandwidth.

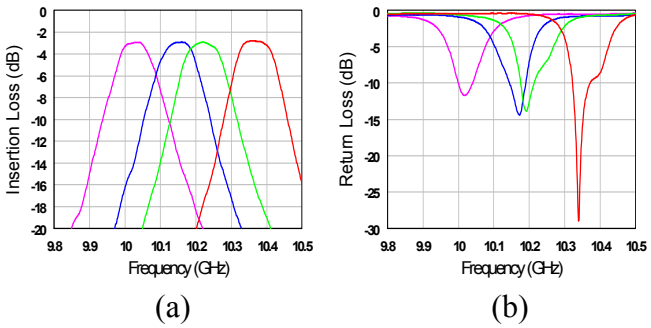

Fig.8. Measured (a) insertion loss and (b) return loss of fixed filters.

TABLE I
MEASURED PERFORMANCE OF FIXED FILTERS

State	f_0 (GHz)	S_{21} (dB)	FBW (%)	Q_U
00	10.37	2.7	0.48	510
01	10.22	2.7	0.36	651
10	10.15	2.6	0.44	531
11	10.03	2.5	0.41	576

B. Tunable Filters

S-parameter measurements were taken on an Anritsu vector network analyzer model 37247D calibrated via an SOLT-type calibration using Agilent's precision 3.5 mm 85033E calibration kit. Measurement results indicate the filter's center frequencies range from 10.12 GHz to 10.33 GHz with bandwidths of 44 MHz – 69 MHz (0.42% - 0.67%). Insertion losses ranged from 4.7 dB to 5.8 dB depending on the filter state with Q_u ranging from 169-319. Measured insertion loss

and return loss are shown in Fig. 9 and summarized in Table II. Both forward and reverse return losses are plotted because of the asymmetry resulting from a fabrication defect. This asymmetry makes bandwidth determination according to 10 dB return loss invalid, therefore bandwidths are defined by 0.5 dB ripple bandwidth. Copper tape was used to form the missing center metal septum (fabrication defect). Suspected implications of the copper tape septum include a narrowing of the pass band as only one of the two poles is apparent and a frequency shift to higher frequencies as the exact impedance of the septum and length of the resonator sections is unknown.

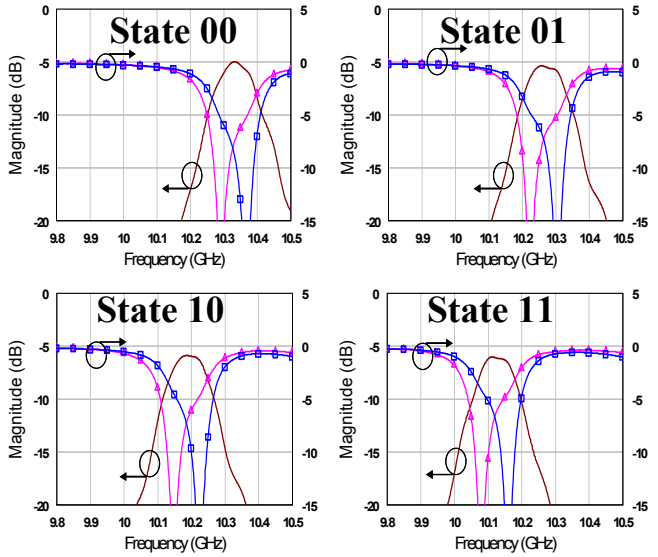

Fig.9. Measured S_{21} (—), S_{11} (—Δ—), and S_{22} (—□—) for (a) filter state "*00*", (b) filter state "*01*", (c) filter state "*10*", and (d) filter sate "*11*."

TABLE II
MEASURED PERFORMANCE OF MEMS-TUNABLE FILTER

State	f_0 (GHz)	S_{21} (dB)	FBW (%)	Q_U
00	10.33	4.7	0.42	319
01	10.26	5.1	0.67	185
10	10.19	5.7	0.64	176
11	10.12	5.8	0.65	169

V. DISCUSSION OF RESULTS

Differences in unloaded quality factors between the tunable and fixed filter demonstrations are thought to be due to a combination of bias lines, wirebonds, and non-integrated MEMS switches. It is believed that the tunable filter performance can be improved to the level of the fixed filters ($Q > 500$) with careful routing of the bias lines. Even better performance could be obtained with the monolithic integration of the MEMS switches and the use of a low-loss "hard-board" material, such as quartz.

ACKNOWLEDGMENTS

This work was supported by DARPA under the SBIR contract W31P4Q-08-C-0230. Approved for public release, distribution unlimited.

REFERENCES

[1] Charles L. Goldsmith, "MEMS Communications on a Credit Card: The RF MEMS Revolution, Defense Science & Technology seminar on Emerging Technologies: MEMS Applications for the individual Warfighter, Crystal City, VA, September 10, 1999.

[2] Dussopt, L.; Rebeiz, G.M., "Intermodulation distortion and power handling in RF MEMS switches, varactors, and tunable filters," *IEEE Trans. Microw. Theory Tech*, vol.51, no.4, pp. 1247-1256, Apr 2003.

[3] Abbaspour-Tamijani, A.; Dussopt, L.; Rebeiz, G.M., "Miniature and tunable filters using MEMS capacitors," *IEEE Trans. Microw. Theory Tech*, vol.51, no.7, pp. 1878-1885, July 2003.

[4] Yan, W. D.; Mansour, R. R., "Tunable Dielectric Resonator Bandpass Filter with Embedded MEMS Tuning Elements," *IEEE Trans. Microw. Theory Tech*, vol.55, no.1, pp.154-160, Jan. 2007.

[5] Entesari, K.; Rebeiz, G.M., "A 12–18-GHz Three-Pole RF MEMS Tunable Filter," *IEEE Trans. Microw. Theory Tech*, vol.53, no.8, pp. 2566-2571, Aug. 2005.

[6] Fouladi, S.; Bakri-Kassem, M.; Mansour, R.R., "An Integrated Tunable Band-Pass Filter Using MEMS Parallel-Plate Variable Capacitors Implemented with 0.35µm CMOS Technology," *IEEE MTT-S Microw. Symp. Dig., 2007,* pp.505-508.

[7] Reines, Isak; Brown, Andrew; El-Tanani, Mohammed; Grichener, Alex; Rebeiz, Gabriel, "1.6-2.4 GHz RF MEMS tunable 3-pole suspended combline filter," *IEEE MTT-S Microw. Symp. Dig., 2008,*133-136.

[8] Ong, C.; Okoniewski, M., "MEMS-Switchable Coupled Resonator Microwave Bandpass Filters," *IEEE Trans. Microw. Theory Tech*, vol.56, no.7, pp.1747-1755, July 2008.

[9] Levy, R., "Theory of Direct-Coupled-Cavity Filters," *IEEE Trans. Microw. Theory Tech*, vol.15, no.6, pp. 340-348, Jun 1967.

[10] Yi-Chi Shih, "Design of Waveguide E-Plane Filters with All-Metal Inserts," *IEEE Trans. Microw. Theory Tech* , vol.32, no.7, pp. 695-704, Jul 1984.

[11] D. W. Kim and J.H. Lee, "A partial H-plane waveguide as a new type of compact waveguide," *Microw. Opt. Technol. Lett.*, vol. 43, no. 5, pp. 351-353, May 2004.

[12] Kim, D.-W.; Kim, D.-J.; Lee, J.-H., "Compact Partial H-Plane Filters," *IEEE Trans. Microw. Theory Tech*, vol.54, no.11, pp.3923-3930, Nov. 2006.

[13] Z.J. Yao, S. Chen, S. Eshelman, D. Denniston, and C. Goldsmith, "Micromachined low-loss microwave switches," *J. Microelectromech. Syst.*, vol. 8, no. 2, pp. 129-134, June 1999.